Luminescent $(Er,Ho)_2O_3$ thin films by ALD to enhance the performance of silicon solar cells

Amr Ghazy,[a] Muhammad Safdar,[a] Mika Lastusaari,[b] Arto Aho,[c] Antti Tukiainen,[c] Hele Savin,[d] Mircea Guina,[c] Maarit Karppinen*[a]

[a] Department of Chemistry and Materials Science, Aalto University, FI-00076 Espoo, Finland

[b] Department of Chemistry, University of Turku, FI-20014 Turku, Finland

[c] Optoelectronic Research Centre, Tampere University, Finland

[d] Department of Electronics and Nanoengineering, Aalto University, FI-00076 Espoo, Finland

Email: maarit.karppinen@aalto.fi

Keywords: c-Si solar cell; luminescence; upconversion; atomic layer deposition ; photonics

ToC Graphic:

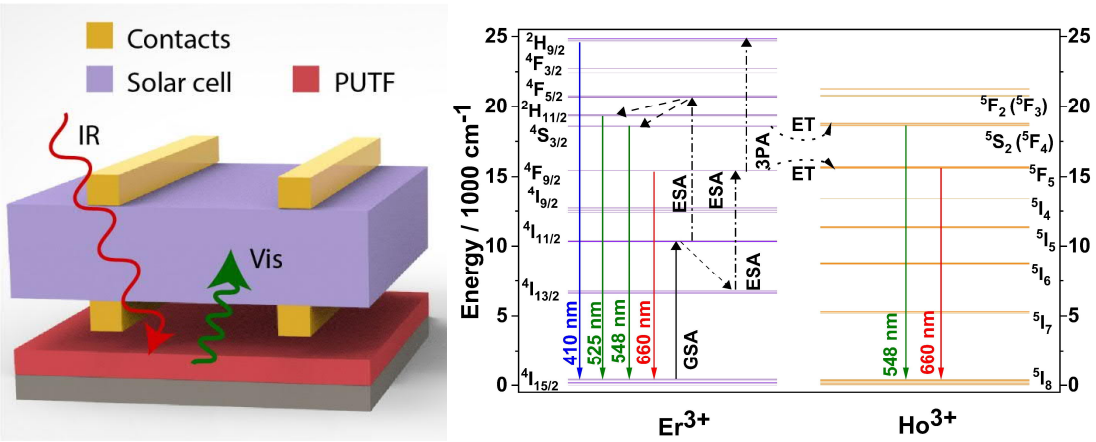

Photon-upconverting thin films are combined with bifacial c-Si solar cell technology to harvest energy of transmitted IR photons, which increased short-circuit current density of the cell by 3%.

Abstract

We have fabricated luminescent $(Er,Ho)_2O_3$ thin films by atomic layer deposition (ALD) and studied their capability to enhance the performance of state-of-the-art single-junction c-Si bifacial solar cells. The films convert IR photons (e.g. 1523 nm) by three- and two-photon upconversion process to emit visible-light in the 400-700 nm range. When the films were coupled with solar cells, ~3% improvement in the short-circuit current density (620±5 to 638±5 $mAcm^{-2}$) was recorded under a simulated solar excitation equivalent to 16 suns. These findings highlight a potential of ALD for the design and fabrication of luminescent coatings for practical solar cell devices.

Introduction

A majority of the mainstream solar cell technologies rely mainly on the visible portion of the solar spectrum, the exact wavelength range depending on the bandgap of the semiconductor they are based on. The high-energy photons are missed as thermalization losses, which are up to 33% for a single-junction Si solar cell [1]. On the other hand, about 19% losses originate due to poor utilization of the low-energy (infrared, IR) radiation by Si, hence named transmission losses. These combined loss mechanisms are the major obstacle to the further improvements of solar cell efficiencies, limiting the performance to the Shockley–Queisser (SC) limit (~30% for c-Si PV cells), particularly in the single-junction solar cells [2].

The performance of Si PV cells could be enhanced by integrating in them components capable of converting high and/or low energy photons into visible (Vis) light, thus extending the range of usable solar light. Computational studies have indeed predicted up to 47.6% efficiency for c-Si PV cells coupled with IR-to-Vis upconverters, under non-concentrated sunlight [3]. Upconversion (UC) is an anti-Stokes process in which two or more low-energy photons are sequentially absorbed via an intermediate long-lived excited state, resulting in a higher excited state that emits a higher energy photon. On the other hand, the high-to-low energy photon-conversion can be categorized as downconversion or downshifting. In downconversion, a UV photon is absorbed to emit at least two low-energy Vis photons, whereas in downshifting, absorption of a UV photon leads to emission of a single Vis photon. Downconversion in solar cells was theoretically shown to lead to a conversion

efficiency of up to 39.6% [4], whereas downshifting can effectively enhance the overall conversion efficiency of the Si solar cells, by ca. 10% [5].

Trivalent lanthanide ions (Ln^{3+}) make the most promising class of luminescent (up- and down-converting/shifting) materials for enhancing solar cell performance owing to their ladder-like energy levels and stable emission under relatively low excitation power density [6]. In early works, UC $NaYF_4:Er^{3+}$ microcrystals were used to boost the efficiency of bifacial c-Si solar cells [7–9]. A bifacial c-Si cell was placed above a 20% Er^{3+}-doped $NaYF_4$ UC layer; when illuminated by a 6 mW 1523 nm laser, a maximum external quantum efficiency of 3.4% was measured [9]. Fischer *et al*. attached a UC layer of β-$NaYF_4$ doped with 25% Er^{3+} embedded in the polymer perfluorocyclobutyl to the rear side of a bifacial Si solar cell [10], and recorded an increase of the short-circuit current density (I_{sc}) of 13.1 $mAcm^{-2}$ due to the UC of sub-band-gap photons, under a solar concentration of 210 suns. Upconversion through Ho^{3+},Yb^{3+} co-doping has been studied in a fluoroindate glass placed at the rear of a bifacial Si solar cell [11]. The efficiency enhancement due to the UC was determined to be 0.003%. Later, preparation of Ln-based upconverting nanoparticles (UCNPs) through wet-chemical techniques emerged as a superior approach. For example, the energy conversion efficiency of organic solar cells could be enhanced by ca. 13% (under AM1.5 G illumination of 100 $mWcm^{-2}$ and a 980 nm laser) by $NaYF_4:Yb^{3+},Er^{3+}$ UCNP coatings [12]. For perovskite solar cells, even more significant enhancements have been reported [13]. Most recently, Guo *et al*. recorded 15.7% increase of efficiency for their perovskite solar cells containing tri-doped (Yb^{3+},Er^{3+},Sc^{3+}) UCNPs [14]. In the case of dye-sensitized solar cells, Ho^{3+},Yb^{3+} based UCNPs have contributed to a 37% improvement of the overall energy conversion efficiency, under AM1.5G light [15].

The aforementioned cases point to the lower performance improvements so far achieved for the Si solar cells in comparison to the various wide-bandgap PV devices, i.e., perovskite, dye-sensitized and organic solar cells [16]. This is predominantly due to the narrow bandgap (1.1 eV) of Si which allows it to absorb well up to ca. 1100 nm. The commonly employed Ln ions, Yb^{3+} and Nd^{3+}, absorb strongly around 980 nm and 808 nm, respectively, but this wavelength range is already well absorbed by Si itself; hence, incorporation of these ions into UC materials is not much beneficial for c-Si solar cells. Instead, by selecting Ln dopants with absorption >1100 nm, e.g. Er^{3+} and Ho^{3+}, could possibly be more useful because these ions absorb in the 1450–1580 nm and 1150–1230 nm ranges, respectively [17].

Emission bands are mostly in the Vis range: Er^{3+} emits strong luminescence at 980 nm, 540 nm, and 650 nm, and Ho^{3+} at 910 nm and 650 nm [18]. The c-Si solar cells exhibit high spectral responses towards these IR wavelengths. Hence, a combination of Er^{3+} and Ho^{3+} ions in an UC material intuitively fits the needs of Si based solar cells. Moreover, applying the UC material as a high-quality conformal coating, would offer an additional benefit to realize the maximal improvements for the c-Si PV cells. The challenge with the use of conventional Ln-doped materials is that their application as thin films either requires suitably index-matched matrix materials (in the case of powder materials)[10] or spin coating, spray drying or electrodeposition methods (for UCNPs) [19], which leads to poor control over the film thickness and conformality. Thus, alternate approaches to prepare UC thin films/coatings are desired.

Atomic layer deposition (ALD) is the state-of-the-art industrial thin film technology for advanced inorganic thin films [20]. In ALD, mutually reactive gaseous/vaporized metal and co-reactant precursor molecules are sequentially pulsed into the reactor chamber; this enables – through self-limiting gas-surface chemical reactions – the fabrication of high-quality thin films with atomic level accuracy. The thus grown thin films are precisely thickness-controlled, conformal, uniform over large-area and complex substrate surfaces, and free from solvent impurities. Most importantly, the technique has been used to deposit Ln-based thin films showing interesting photoluminescence [21–27] and photon-upconversion [28–30] properties. The examples of UC thin films prepared by ALD remain scarce, despite the potential that the ALD technique promises for the material fabrication. Here, we introduce ALD-fabricated luminescent Ln-based thin films, which when coupled with a bifacial c-Si solar cell, result in ca. 3% increase in the short-circuit current density.

Materials and methods

Our luminescent $(Er,Ho)_2O_3$ thin films were composed of 95% Er^{3+} and 5% Ho^{3+}. To obtain these mixed $(Er,Ho)_2O_3$ films, we employed in-house synthesized $Er(thd)_3$ and $Ho(thd)_3$ (thd = 2,2,6,6-tetramethyl-3,5-heptanedione) precursor powders, which were mechanically mixed at the desired ratio and thoroughly homogenized in a mortar and pestle. Ozone (O_3) was used as the source of oxygen. The thin-film depositions were carried out in a commercial flow-type hot-wall ALD reactor (F-120 by ASM Microchemistry Ltd.) at 300 °C deposition temperature. The reactor pressure was maintained

between 3-6 mbar and nitrogen (>99.999%; Schmidlin UHPN 3000 N_2 generator) was used both as the purging and carrier gas. The mixed $Er(thd)_3/Ho(thd)_3$ precursor powder was kept in an open glass crucible inside the reactor at 130 °C, while O_3 was pulsed at room temperature. The pulse/purge lengths for the mixed Ln precursor were 1.5s/2s, while for O_3 2.5s/3s. The process parameters were obtained from previously known Ln-oxide thin films produced by ALD [31].

The films were deposited on Si(100) substrates (4×4 cm^2 and 15×15 mm^2). They were characterized for crystal structure by grazing incidence X-ray diffraction (GIXRD; X'Pert Pro MPD, PANalytical; Cu K_α; step size 0.02º, 16.5 s time per step). The thickness of the films was verified with X-ray reflectivity (XRR; X'Pert Pro MPD, PANalytical; Cu K_α; step size 0.050º, 3.5 s per step). The UC measurements were carried out using AvaSpec- HS-TEC CCD spectrometer and Optical Fiber Systems IFC-975-008 NIR laser (6 W, 974 nm). In the excitation path, a 900 nm long-pass filter (Edmund Optics) was used to cut off wavelengths lower than NIR. The emitted light was collected at 90° angle to the excitation and directed through a 900 nm filter (Newport, 10SWF-900-B) to exclude the scattered excitation radiation. An optical fiber with 600 μm diameter was used as an emission light path between the sample compartment and the detector. All spectra were measured at room temperature.

Results and discussions

The UC films of different thicknesses, i.e. 30, 45 and 60 nm, were fabricated using ALD. The crystal structure of the films and film thickness were confirmed by GIXRD and XRR. Figure 1a indicates that our polycrystalline $(Er,Ho)_2O_3$ films were of the cubic Ln_2O_3 phase, as expected [30]. The film growth rate expressed as the GPC (growth per cycle) value was found to be ca. 0.28 Å/cycle, which matches with the literature values for ALD-grown Ln_2O_3 films [31]. Hence, a deposition performed using 2000 ALD cycles resulted in ca. 60 nm thick film for which the density and surface roughness values obtained by fitting the XRR curve (Figure 1b) were found to be 8.022 gcm^{-3} and 0.6 nm, respectively.

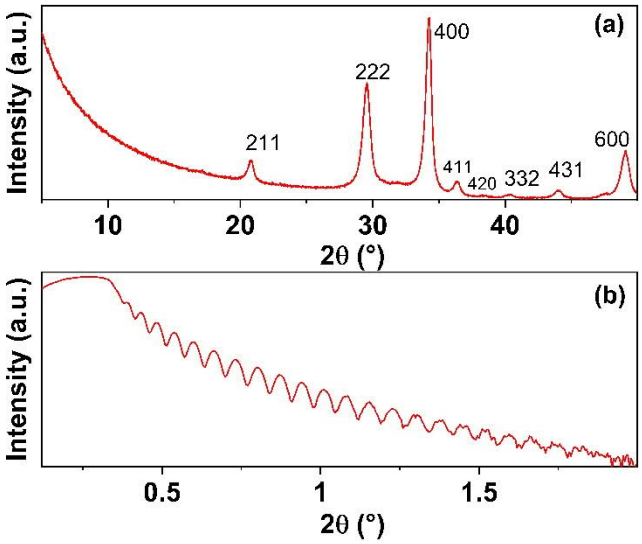

Figure 1. (a) GIXRD (Miller indices for the cubic Ln_2O_3 phase) and (b) XRR patterns for a representative ALD grown $(Er,Ho)_2O_3$ thin film.

Since the mixture of Er^{3+} and Ho^{3+} ions could be expected to produce UC emission [32], we performed upconversion luminescence measurements to check the luminescence emission from our $(Er,Ho)_2O_3$ films. The NIR absorption bands of Er^{3+} are peaked around 980 nm and 1523 nm. Our actual interest for the practical application is in the absorption in 1523 nm range. However, due to the lack of the 1523 nm laser source, we selected a 974 nm laser as an excitation source to only confirm the IR absorption of the films. Upon excitation at 974 nm, our $(Er,Ho)_2O_3$ film showed green and red UC emission that appeared green to the naked eye. Figure 2 shows the emission spectrum for a 45 nm thick film, and a suggested mechanism of the energy transfer processes, which is in accord with the literature.[32] Emissions at 525, 548 and 660 nm correspond to Er^{3+}:$^2H_{11/2} \rightarrow {}^4I_{15/2}$, Er^{3+}:$^4S_{3/2} \rightarrow {}^4I_{15/2}$ + Ho^{3+}:$^5S_2(^5F_4) \rightarrow {}^5I_8$, and Er^{3+}:$^4F_{9/2} \rightarrow {}^4I_{15/2}$ + Ho^{3+}:$^5F_5 \rightarrow {}^5I_8$ transitions, respectively. However, because no signal was observed at ca. 750 nm, where the $^5I_4 \rightarrow {}^5I_8$ and $^5S_2,{}^5F_4 \rightarrow {}^5I_7$ transitions of Ho^{3+} should be present, it seems that the contribution of Ho^{3+} is either small or non-existent in the UC emission spectrum with 974 nm excitation. This does not rule out the fact that Ho^{3+} could participate in the UC excitation process. In addition to green and red emission, the films also emitted blue photons, peaked around 410 nm due to the Er^{3+}:$^2H_{9/2} \rightarrow {}^4I_{15/2}$ transitions.

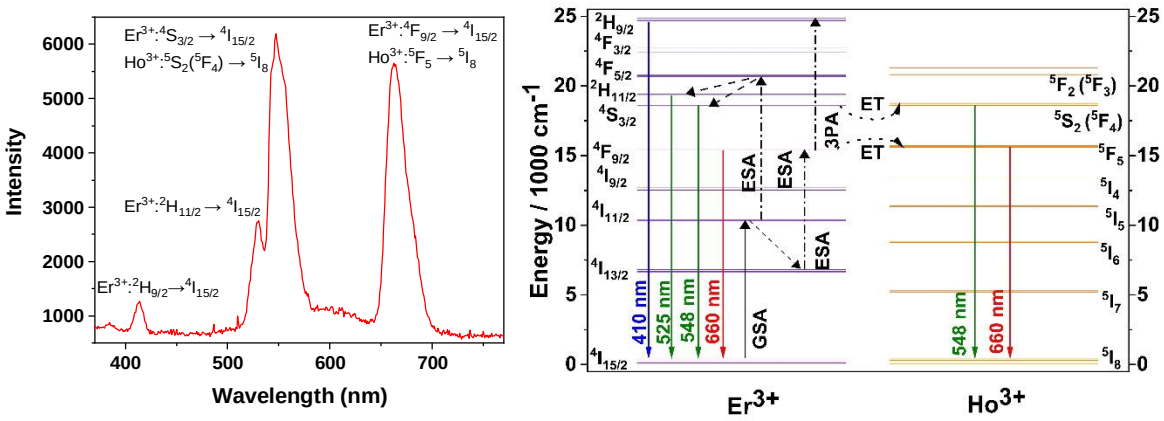

Figure 2. Left: Emission spectra of the $(Er,Ho)_2O_3$ thin films under 974 nm NIR laser excitation. Right: Suggested photon absorption, energy transfer and UC photon emission mechanism.

We determined absorption properties of our test c-Si bifacial solar cell by measuring its transmission spectrum (Figure 3a). The cell clearly starts to suffer from significant transmission losses at wavelengths >1000 nm. Figure 3(b) shows the external quantum efficiency (EQE) of the cell measured from the rear side.

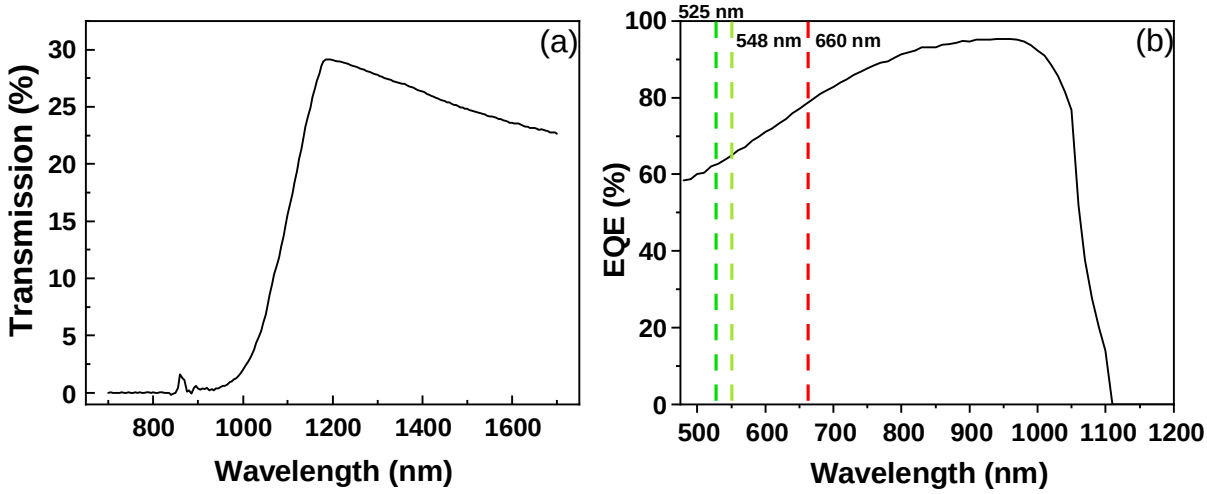

Figure 3. (a) Transmission spectrum of the state-of-the-art bifacial solar cells that shows energy losses due to poor absorption by the cell in the IR region. (b) EQE of the bifacial solar cell measured from the rear side.

We then coupled our $(Er,Ho)_2O_3$ thin films of the different thicknesses (30, 45 and 60 nm) with the solar cell, as illustrated in Figure 4, to study the improvement in short-circuit current density (J_{sc}) of the cell. Since the solar cell was primary designed for one sun operation, we used I_{sc} for the evaluation

of the different thin film structures. We assumed linear dependence between I_{sc} values and incoming photon flux, which is a valid assumption for high quality solar cell materials. The thin film substrates were placed underneath the c-Si solar cell at a distance of 1.0 mm. The backside of the cell was only partially illuminated. The total backside area for illumination was ca. 14 mm x 8.3 mm (1.16 cm^2).

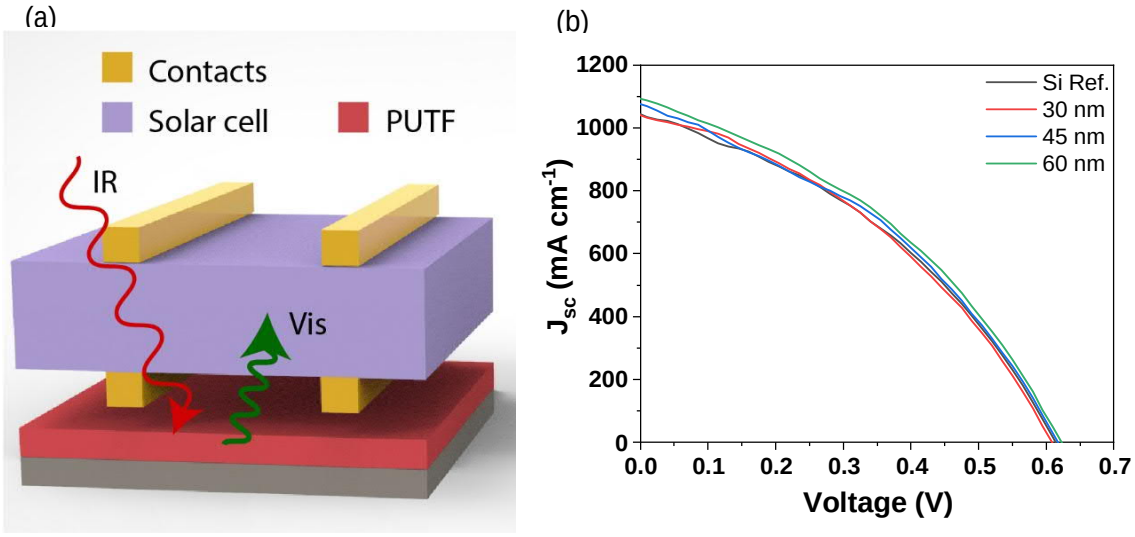

Figure 4. (a) Schematic diagram showing the physically coupled thin film on Si substrate, to a c-Si bifacial solar cell. (b) Current density-voltage plot of the c-Si bifacial solar cell 30, 45 and 60 nm thick $(Er,Ho)_2O_3$ films, as well as bare, reference Si substrate.

Figure 4(a) illustrates the physically coupled UC thin film and bifacial solar cell. The IV-characteristics were measured using commercial steady-state CPV solar simulator (7 kW TriSol system from OAI Corporation). The spectrum fits closely to ASTM G173-3 AM1.5D (1000 Wm^{-2}) standard. For the measurement, fixed concertation of approximately 16 suns was used. We did not observe any change in the I_{sc} under nonconcentrated or less concentrated conditions. Figure 4(b) shows the J_{sc}-V curve of the solar cell when coupled with the thin films. The short-circuit current density of our c-Si bifacial solar cell increased by 0%, 1.5% and 2.8% for films of 30, 45 and 60 nm thickness, respectively. Standard deviation for the short circuit current values was estimated to be +/- 1 percentage points. If it would have been technically possible to measure the solar cell with the full backside illumination, 0%, 2.6% and 4.8% enhancements could be expected with the corresponding film thicknesses, the busbar coverage (0.0174 cm^2) on the backside was taken into account. This proof-of-concept study clearly demonstrates advantage that our ALD $(Er,Ho)_2O_3$ thin films offer to the existing solar cell

technology, without requiring any alteration of the solar cell architecture. We want to note here that the grid design and the heat conduction (only free air convection cooling) was not optimized for 16 suns. These factors reduce the fill factor and open circuit voltages of the c-Si solar cell significantly. We believe that the improvement in the I_{sc} is linked to the UC luminescence emission form the $(Er,Ho)_2O_3$ films, towards the rear of the bifacial Si solar cell. Further studies related to the complete optimization of the ALD thin-film fabrication process, angle and powder dependent UC emission and detailed investigation of the performance improvement is currently being performed.

Conclusions

We fabricated high-quality polycrystalline luminescent $(Er,Ho)_2O_3$ thin films by ALD. The films emitted blue, green and red photons upon excitation by 974 nm NIR laser irradiation. When these films were combined with c-Si bifacial solar cells, a ~3% increase in the I_{sc} of the cell was recorded. These findings hold a great promise for other solar cell materials as well, such as perovskite and dye-sensitized solar cells, which tend to suffer greater transmission losses. The conformal, solvent-free growth of Ln-based UC thin films by ALD can unlock unique features and benefits for practical solar cell devices.

Acknowledgements

We thank Iris Mack, Department of Electronics and Nanoengineering, Aalto University, for her kind support. Funding was received from European Research Council for the Advanced Grant Projects LAYERENG-HYBMAT (339478) and AMETIST (695116), and also from Academy of Finland (296299). The authors also acknowledge the funding provided by the Academy of Finland Flagship Programme, Photonics Research and Innovation (PREIN), decision number: 320167 and 340168, and the use of the RawMatTERS Finland Infrastructure (RAMI) at Aalto University. Amr Ghazy acknowledges Jenny & Antti Wihuri Foundation for financial support.

References

[1] O.E. Semonin, J.M. Luther, M.C. Beard, Quantum dots for next-generation photovoltaics, Mater. Today 15 (2012) 508–515. https://doi.org/10.1016/S1369-7021(12)70220-1.

[2] J.C. Goldschmidt, S. Fischer, Upconversion for photovoltaics - a review of materials, devices and concepts for performance enhancement, Adv. Opt. Mater. 3 (2015) 510–535. https://doi.org/10.1002/adom.201500024.

[3] T. Trupke, M.A. Green, P. Würfel, Improving solar cell efficiencies by up-conversion of sub-

band-gap light, J. Appl. Phys. 92 (2002) 4117–4122. https://doi.org/10.1063/1.1505677.

[4] T. Trupke, M.A. Green, P. Würfel, Improving solar cell efficiencies by down-conversion of high-energy photons, J. Appl. Phys. 92 (2002) 1668–1674. https://doi.org/10.1063/1.1492021.

[5] W.G.J.H.M. Van Sark, Enhancement of solar cell performance by employing planar spectral converters, Appl. Phys. Lett. 87 (2005) 1–3. https://doi.org/10.1063/1.2099532.

[6] G. Chen, H. Ågren, T.Y. Ohulchanskyy, P.N. Prasad, Light upconverting core-shell nanostructures: Nanophotonic control for emerging applications, Chem. Soc. Rev. 44 (2015) 1680–1713. https://doi.org/10.1039/c4cs00170b.

[7] A. Shalav, B.S. Richards, T. Trupke, K.W. Krämer, H.U. Güdel, Application of $NaYF_4:Er^{3+}$ up-converting phosphors for enhanced near-infrared silicon solar cell response, Appl. Phys. Lett. 86 (2005) 013505. https://doi.org/10.1063/1.1844592.

[8] S. Fischer, J.C. Goldschmidt, P. Löper, G.H. Bauer, R. Brüggemann, K. Krämer, D. Biner, M. Hermle, S.W. Glunz, Enhancement of silicon solar cell efficiency by upconversion: Optical and electrical characterization, J. Appl. Phys. 108 (2010) 044912. https://doi.org/10.1063/1.3478742.

[9] A. Shalav, B.S. Richards, K. Krämer, H. Güdel, Improvements of an up-conversion $NaYF_4:Er^{3+}$ phosphor/silicon solar cell system for an enhanced response in the near-infrared, Conf. Rec. IEEE Photovolt. Spec. Conf. (2005) 114–117. https://doi.org/10.1109/pvsc.2005.1488082.

[10] S. Fischer, A. Ivaturi, B. Frohlich, M. Rudiger, A. Richter, K.W. Kramer, B.S. Richards, J.C. Goldschmidt, Upconverter silicon solar cell devices for efficient utilization of sub-band-gap photons under concentrated solar radiation, IEEE J. Photovoltaics 4 (2014) 183–189. https://doi.org/10.1109/JPHOTOV.2013.2282744.

[11] F. Lahoz, C. Pérez-Rodríguez, S.E. Hernández, I.R. Martín, V. Lavín, U.R. Rodríguez-Mendoza, Upconversion mechanisms in rare-earth doped glasses to improve the efficiency of silicon solar cells, Sol. Energy Mater. Sol. Cells 95 (2011) 1671–1677. https://doi.org/10.1016/j.solmat.2011.01.027.

[12] F. Wang, X.Y. Yang, M.S. Niu, L. Feng, C.K. Lv, K.N. Zhang, P.Q. Bi, J. Yang, X.T. Hao, Enhancing light harvesting and charge transport in organic solar cells via integrating lanthanide-doped upconversation materials, J. Phys. D. Appl. Phys. 51 (2018). https://doi.org/10.1088/1361-6463/aac568.

[13] Y. Wu, X. Ding, X. Shi, T. Hayat, A. Alsaedi, Y. Ding, L.E. Mo, S. Dai, Highly efficient infrared light-converting perovskite solar cells: direct electron injection from $NaYF_4:Yb^{3+},Er^{3+}$ to the TiO_2, ACS Sustain. Chem. Eng. 6 (2018) 14004–14009. https://doi.org/10.1021/acssuschemeng.8b02500.

[14] Q. Guo, J. Wu, Y. Yang, X. Liu, J. Jia, J. Dong, Z. Lan, J. Lin, M. Huang, Y. Wei, Y. Huang, High performance perovskite solar cells based on β-$NaYF_4:Yb^{3+}/Er^{3+}/Sc^{3+}$@$NaYF_4$ core-shell upconversion nanoparticles, J. Power Sources 426 (2019) 178–187. https://doi.org/10.1016/j.jpowsour.2019.04.039.

[15] J. Yu, Y. Yang, R. Fan, D. Liu, L. Wei, S. Chen, L. Li, B. Yang, W. Cao, Enhanced near-infrared to visible upconversion nanoparticles of Ho^{3+}-Yb^{3+}-F- tri-doped TiO_2 and its application in dye-sensitized solar cells with 37% improvement in power conversion efficiency, Inorg. Chem. 53 (2014) 8045–8053. https://doi.org/10.1021/ic501041h.

[16] A. Shalav, B.S. Richards, T. Trupke, K.W. Krämer, H.U. Güdel, Application of $NaYF_4$:Er^{3+} up-converting phosphors for enhanced near-infrared silicon solar cell response, Appl. Phys. Lett. 86 (2005) 013505. https://doi.org/10.1063/1.1844592.

[17] X. Cheng, H. Ge, Y. Wei, K. Zhang, W. Su, J. Zhou, L. Yin, Q. Zhan, S. Jing, L. Huang, Design for brighter photon upconversion emissions via energy level overlap of lanthanide ions, ACS Nano 12 (2018) 10992–10999. https://doi.org/10.1021/acsnano.8b04988.

[18] Y. Shang, S. Hao, C. Yang, G. Chen, Enhancing solar cell efficiency using photon upconversion materials, Nanomaterials 5 (2015) 1782–1809. https://doi.org/10.3390/nano5041782.

[19] H. Jia, C. Xu, J. Wang, P. Chen, X. Liu, J. Qiu, Synthesis of $NaYF_4$:Yb-Tm thin film with strong NIR photon up-conversion photoluminescence using electro-deposition method, CrystEngComm 16 (2014) 4023–4028. https://doi.org/10.1039/c4ce00078a.

[20] S.M. George, Atomic layer deposition: An overview, Chem. Rev. 110 (2010) 111–131. https://doi.org/10.1021/cr900056b.

[21] Z. Giedraityte, P. Sundberg, M. Karppinen, Flexible inorganic–organic thin film phosphors by ALD/MLD, J. Mater. Chem. C 3 (2015) 12316–12321. https://doi.org/10.1039/C5TC03201F.

[22] Z. Giedraityte, J. Sainio, D. Hagen, M. Karppinen, Luminescent metal-nucleobase network thin films by atomic/molecular layer deposition, J. Phys. Chem. C 121 (2017) 17538–17545. https://doi.org/10.1021/acs.jpcc.7b06129.

[23] M.N. Getz, P.A. Hansen, Ø.S. Fjellvåg, M.A.K. Ahmed, H. Fjellvåg, O. Nilsen, Intense NIR emission in YVO_4:Yb^{3+} thin films by atomic layer deposition, J. Mater. Chem. C 5 (2017) 8572–8578. https://doi.org/10.1039/c7tc02135f.

[24] M. Getz, P.A. Hansen, M.A.K. Ahmed, H. Fjellvåg, O. Nilsen, Luminescent $YbVO_4$ by atomic layer deposition, Dalt. Trans. 46 (2017) 3008–3013. https://doi.org/10.1039/c7dt00253j.

[25] P.A. Hansen, H. Fjellvåg, T.G. Finstad, O. Nilsen, Luminescence properties of europium titanate thin films grown by atomic layer deposition, RSC Adv. 4 (2014) 11876–11883. https://doi.org/10.1039/c3ra47469k.

[26] P.-A. Hansen, H. Fjellvåg, T.G. Finstad, O. Nilsen, Luminescence properties of lanthanide and ytterbium lanthanide titanate thin films grown by atomic layer deposition, J. Vac. Sci. Technol. A 34 (2016) 01A130. https://doi.org/10.1116/1.4936389.

[27] V. Kiisk, A. Tamm, K. Utt, J. Kozlova, H. Mändar, L. Puust, J. Aarik, I. Sildos, Photoluminescence of atomic layer deposited ZrO_2:Dy^{3+} thin films, Thin Solid Films 583 (2015) 70–75. https://doi.org/10.1016/j.tsf.2015.03.041.

[28] Z. Giedraityte, M. Tuomisto, M. Lastusaari, M. Karppinen, Three- and two-photon NIR-to-Vis

(Yb,Er) upconversion from ALD/MLD-fabricated molecular hybrid thin films, ACS Appl. Mater. Interfaces 10 (2018) 8845–8852. https://doi.org/10.1021/acsami.7b19303.

[29] M. Tuomisto, Z. Giedraityte, L. Mai, A. Devi, V. Boiko, K. Grzeszkiewicz, D. Hreniak, M. Karppinen, M. Lastusaari, Up-converting ALD/MLD thin films with Yb^{3+},Er^{3+} in amorphous organic framework, J. Lumin. 213 (2019) 310–315. https://doi.org/10.1016/j.jlumin.2019.05.028.

[30] M. Tuomisto, Z. Giedraityte, M. Karppinen, M. Lastusaari, Photon up-converting $(Yb,Er)_2O_3$ thin films by atomic layer deposition, Phys. Status Solidi - RRL 11 (2017) 1700076. https://doi.org/10.1002/pssr.201700076.

[31] M. Leskelä, K. Kukli, M. Ritala, Rare-earth oxide thin films for gate dielectrics in microelectronics, J. Alloys Compd. 418 (2006) 27–34. https://doi.org/10.1016/j.jallcom.2005.10.061.

[32] X. Zhang, T. Xu, S. Dai, Q. Nie, X. Shen, L. Lu, X. Zhang, Investigation of energy transfer and frequency upconversion in Er^{3+}/Ho^{3+} co-doped tellurite glasses, J. Alloys Compd. 450 (2008) 306–309. https://doi.org/10.1016/j.jallcom.2006.10.097.